

Stem Cell-Based Microphysiological Osteochondral System to Model Tissue Response to Interleukin-1 β

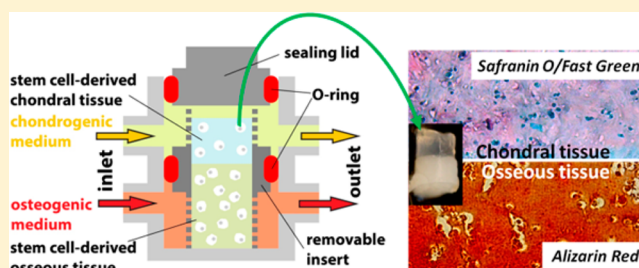
Hang Lin,^{†,§} Thomas P. Lozito,^{†,§} Peter G. Alexander,^{†,§} Riccardo Gottardi,^{†,‡} and Rocky S. Tuan^{*,†}

[†]Center for Cellular and Molecular Engineering, Department of Orthopaedic Surgery, University of Pittsburgh School of Medicine, Pittsburgh, Pennsylvania 15219, United States

[‡]Ri. MED Foundation, via Bandiera, 11-90133 Palermo, Italy

ABSTRACT: Osteoarthritis (OA) is a chronic degenerative disease of the articular joint that involves both bone and cartilage degenerative changes. An engineered osteochondral tissue within physiological conditions will be of significant utility in understanding the pathogenesis of OA and testing the efficacy of potential disease-modifying OA drugs (DMOADs). In this study, a multichamber bioreactor was fabricated and fitted into a microfluidic base. When the osteochondral construct is inserted, two chambers are formed on either side of the construct (top, chondral; bottom, osseous) that is supplied by different medium streams. These medium conduits are critical to create tissue-specific microenvironments in which chondral and osseous tissues will develop and mature. Human bone marrow stem cell (hBMSCs)-derived constructs were fabricated *in situ* and cultured within the bioreactor and induced to undergo spatially defined chondrogenic and osteogenic differentiation for 4 weeks in tissue-specific media. We observed tissue specific gene expression and matrix production as well as a basophilic interface suggesting a developing tidemark. Introduction of interleukin-1 β (IL-1 β) to either the chondral or osseous medium stream induced stronger degradative responses locally as well as in the opposing tissue type. For example, IL-1 β treatment of the osseous compartment resulted in a strong catabolic response in the chondral layer as indicated by increased matrix metalloproteinase (MMP) expression and activity, and tissue-specific gene expression. This induction was greater than that seen with IL-1 β application to the chondral component directly, indicative of active biochemical communication between the two tissue layers and supporting the osteochondral nature of OA. The microtissue culture system developed here offers novel capabilities for investigating the physiology of osteochondral tissue and pathogenic mechanisms of OA and serving as a high-throughput platform to test potential DMOADs.

KEYWORDS: osteochondral tissue engineering, osteoarthritis, mesenchymal stem cells, interleukin-1 β , matrix metalloproteinase



INTRODUCTION

Osteoarthritis (OA) is a major cause of disability affecting millions of people worldwide. In the United States alone, the disease affects up to 50–60 million people.^{1,2} To date there are no proven therapies for the prevention or treatment of OA. Pain relief and visco-supplementation are prescribed to attenuate the symptoms of OA until disease progression significantly impairs joint function and joint replacements are required.³ The lack of disease modifying OA drugs (DMOADs) may be a function of incongruence between *in vitro* models of OA and the pathogenesis *in vivo*, and between disease mechanisms in humans and model animals. To overcome these issues, there is increasing momentum to develop human cell-based organotypic models *in vitro* that functionally represent the osteochondral tissue directly affected by OA.

The development of physiologically relevant models requires an understanding of the tissue architecture, physiology, and pathophysiological responses to biochemical (or biophysical) insults. This is especially the case for the osteochondral complex, where the main tissues, cartilage and bone, differ so substantially. Cartilage is composed of a collagen type II/

aggrecan-rich, highly hydrated, viscoelastic, anisotropic matrix that encapsulates chondrocytes within biochemically distinct chondrons.⁴ In contrast, bone is composed of a collagen type I-rich, laminated or woven calcified structure that is much stiffer and encapsulates osteocytes, osteoblasts, and osteoclasts, blood vessels, and nerves.^{5–7} The cartilage and bone are intimately connected at the osteochondral junction (OCJ), a highly organized structure that represents a significant challenge to mimic *in vitro* by tissue engineering. It is composed of distinct, interacting layers that include (epi-to-diaphyseally) deep zone cartilage, a basophilic tidemark, calcified cartilage, the cement line, and the subchondral bone plate.⁸ Interestingly, there is growing evidence of significant biochemical communication

Special Issue: Engineered Biomimetic Tissue Platforms for *in Vitro* Drug Evaluation

Received: February 14, 2014

Revised: May 8, 2014

Accepted: May 15, 2014

Published: May 15, 2014

between cartilage and bone across the OCJ.⁹ In the pathogenesis of OA, changes in the physical linkage between cartilage and bone at the OCJ are critical components of disease progression. These include remodeling of the tidemark, microcracks, and fissures in both tissues and ingrowth from the underlying bone of blood vessels and nerves, all of which may enhance the cartilage-bone crosstalk allowing a better passage of growth factors, cytokines, and signaling molecules.¹⁰ These OCJ changes accelerate cartilage degeneration and are associated with joint pain and disease morbidity, pointing to the need of a better understanding of the complex network of interactions between bone and cartilage in OA.¹⁰

Cartilage and bone exist not only in a different matrix but also in very different biophysical environments. *In vivo*, there is a steep oxygen gradient from bone (essentially normoxic) to cartilage (extremely hypoxic).¹¹ These differences are reflected in the *in vitro* culture systems often used to maintain chondrocytes and osteoblasts. Chondrocytes are best maintained in a “starved” environment: low glucose, serum-free medium supplemented with pyruvate and abundant matrix precursors or -enhancing molecules (proline and ascorbate) in hypoxic conditions.¹² However, osteoblasts are maintained in high glucose, serum-containing medium supplemented with β -glycerol phosphate and vitamin D₃ in normoxic conditions.^{13,14}

With these fundamental environmental differences between chondrocytes and osteoblasts, it is not surprising that OA elicits specific responses from each tissue. OA disease progression is most frequently characterized by a net loss of cartilage matrix that results from an imbalance between cartilage matrix degradation and synthesis by chondrocytes in the cartilage.¹⁵ Progressive chronic destruction of articular cartilage is the most obvious characteristic of OA, and the etiology of the disease is believed to be at the intersection of genetics and abnormal mechanical forces.¹⁶ Therefore, the primary locus of the disease is traditionally presumed to be the cartilage, and as a result, most *in vitro* OA models focus exclusively on cartilage to study OA disease mechanisms and therapeutic intervention. However, there is increasing evidence from *in vivo* and clinical studies that subchondral bone lesions may precede cartilage degeneration, implying that OA is an osteochondral disease and possibly bone dependent.⁵ In addition, it has been often reported that the health of mature articular cartilage *in vitro* is positively impacted by the presence of subchondral bone.¹⁷

Despite these observations, most *in vitro* OA research has not taken into account the effects of bone-cartilage interactions, focusing primarily on cartilage alone. This may account for the dearth of new therapeutics for the prevention and treatment of OA. We theorize that the development of a model system of osteochondral tissue using human cells in a physiologically relevant environment that can accurately replicate *in vivo* osteochondral tissue homeostasis and pathophysiology will lead to greater predictive power in the development of DMOADs. The challenges in developing such a system include: (1) mimicking or inducing production of appropriate extracellular matrix critical to the function of cartilage and bone, (2) replicating the tissue architecture, (3) reconciling the different growth and maintenance conditions of bone and cartilage while promoting their interaction with each other, and (4) replicating the biomechanical environment known to be essential to cartilage and bone health.

Current *in vitro* models to investigate bone-cartilage interactions are mostly limited to cell co-culture systems in which bone and cartilage cells are both exposed to the same

medium,¹⁸ arguably a very distant condition from the *in vivo* environment. Here, we report the development of a bioreactor designed to accommodate the biphasic nature of an osteochondral plug by creating two separate compartments for the “chondral” and “osseous” microenvironments. These are separated only by the tissue itself and are supplied by a microfluidic system. The two microenvironments can be independently controlled and regulated via introductions of bioactive agents or candidate effector cells, and the medium can be individually sampled for compositional assays. The central hypothesis of the study is that a gradient of tissue specific nutrients and conditions is required for the formation and maintenance of the osteochondral tissue. Furthermore, we hypothesize that induction of an OA-like condition in the engineered osseous or the engineered chondral component alone will induce a corresponding OA-like response in the other component. To test these hypotheses, we have generated distinct chondral and osseous zones within the same construct by controlling the different media exposures within the bioreactor. Then, we induced an OA-like response by exposing the osseous or chondral compartments to the pro-inflammatory cytokine (IL-1 β) and assayed the intervening changes in expression and secretion from both the engineered chondral and osseous components.

■ EXPERIMENTAL SECTION

Materials. All chemicals used in this study were purchased from Sigma-Aldrich (St. Louis, MO) unless stated otherwise.

Bioreactor Design and Fabrication. The 3D structures of the bioreactor (Figure 1) were modeled using Magics 14 (Materialise, Belgium). The chamber and insert were fabricated using a stereolithography apparatus (EnvisionTec, Germany) employing e-shell 300 as the resin.

Isolation of hBMSCs. hBMSCs were isolated from the femoral heads of patients undergoing total joint arthroplasty with IRB approval (University of Pittsburgh), cultured and expanded as previously described (Caterson, 2002; Song, 2004). Briefly, bone marrow was flushed out from the trabecular bone of the femoral neck and head using an 18-gauge needle and resuspend in Dulbecco's Minimal Essential Medium (DMEM). The suspension was filtered through a 40 μ m strainer and the flow-through was centrifuged at 300g for 5 min. After the supernatant was discarded, the pellets were suspended using growth medium (GM, α -MEM containing 10% fetal bovine serum (FBS, Invitrogen), 1% antibiotics-antimycotic, and 1.5 ng/mL FGF-2 (RayBiotech, Norcross, GA)), and then plated into 150 cm² tissue culture flasks at a density of 20,000–40,000 nucleated cells/cm², and medium was changed every 3 to 4 days. Once 70% to 80% confluence was reached, cells were passaged. The colony formation and trilineage mesenchymal differentiation capacity of hBMSCs was validated before use (data not shown).¹⁹ All experiments were performed with passage 3 (P3) hBMSCs from 3 patients (3 female patients 44, 52, and 72 years old), which were pooled for use in this study.

Preparation of Photoinitiator LAP. The photoinitiator lithium phenyl-2,4,6-trimethylbenzoylphosphinate (LAP) was synthesized as described by Fairbanks et al.²⁰

Preparation of Methacrylated Gelatin (mGL) and Hyaluronic Acid (mHA). mGL was synthesized by reacting gelatin with methacrylic anhydride (MA) in water according to a procedure previously described.^{21,22} mHA was prepared as previously reported using sodium hyaluronate powder

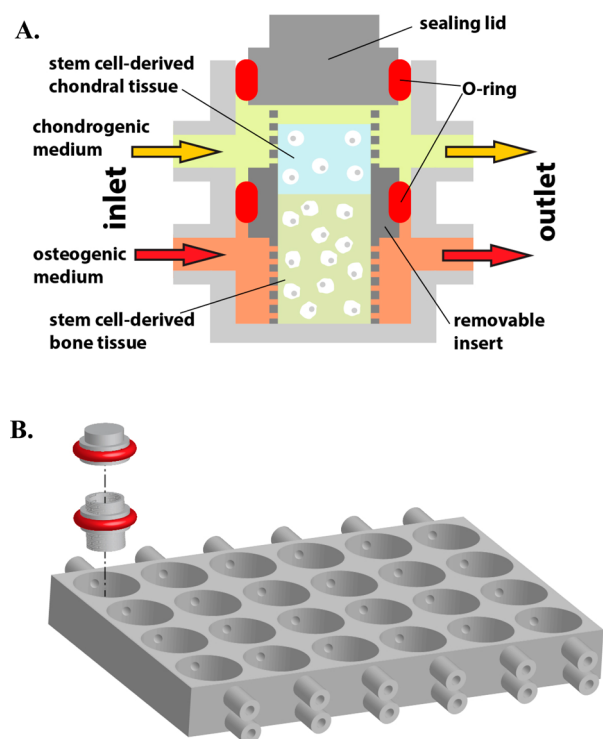


Figure 1. Schematic of the bioreactor for *in vitro* osteochondral engineering. (A) An individual bioreactor composed of the removable insert (dark gray) within a chamber (light gray) of the microfluidic plate (B) and fixed in place with two O-rings. The osteochondral construct within the insert creates the final separation between the upper and lower medium conduits. Opposing gradients of chondrogenic and osteogenic factors and stimulants will aid in forming an interface. (B) A single bioreactor formed by the inset and lid in the context of a 24-well plate. Red circles indicate the O-rings that seal the joint space between lid/insert and chamber.

(research grade, MW \approx 66 kDa, Lifecore).²³ Both mGL and mHA were lyophilized and stored in a desiccator for future use.

Bioreactor System Leak Test. To test medium leakage between (1) the chamber wall and the insert and (2) the insert and scaffold material, the insert was filled with 10% mGL/0.15% LAP in HBSS and cured using a light source producing UV light with wavelength of 390–395 nm. Alexa Fluor 488-conjugated soybean trypsin inhibitor (TI488, 21kd, Molecular Probes, CA) and Alexa Fluor 555-conjugated albumin from bovine serum (BSA) (BSA555, 65kd, Molecular Probes) were diluted in HBSS individually at 10 μ g/mL and then perfused through the top and bottom of bioreactor, respectively, at 1 μ L/min. At different time points, effluent from the upper and

lower medium conduits was collected and the fluorescence intensity at both wavelengths measured using a microplate reader (Synergy HT, BioTek, Winooski, VT). Leaking between top and bottom conduits was estimated by the ratio of TI488 (bottom)/TI488 (top) and BSA555(top)/BSA555 (bottom). Because of the permeable nature of gelatin scaffold used as the scaffold model, leaking was assayed for 24 h only.

Fabrication of Naïve Osteochondral Constructs *in Vitro*. P3 hBMSCs were pelleted and drained completely in order to prevent the unwanted dilution of polymers. Chondrogenic cell suspension: hBMSCs were resuspended in 10% mGL/1% mHA/0.15% LAP (w/v) HBSS solution (pH adjusted to 7.4) at a final density of 20×10^6 /mL (chondrogenic suspension). Osteogenic cell suspension: hBMSCs were resuspended in the 10% mGL/1% hydroxyapatite/0.15% LAP (w/v) HBSS solution (pH was adjusted to 7.4) at a final density of 20×10^6 /mL. Osteochondral construct preparation: First, the insert was placed within a hollow cylindrical well to prevent suspension leaking from the pores in the insert. Second, 60 μ L of osteogenic suspension was pipetted into the insert and cross-linked using the UV light source. After 2 min of UV light exposure, the inset with photopolymerized osseous construct was removed from the chamber. Third, 30 μ L of chondral suspension was added on the top of osseous construct within the same insert and cured for another 2 min. Previous studies have shown cell viability within the scaffold >90% after photo-cross-linking (data not shown).¹⁹ The second round of cross-linking had the added benefit of bonding the osseous and chondral layers together as well, and the fabrication of the osteochondral construct within the insert created a tight seal.

Culture of Osteochondral Constructs *in Vitro*. The inserts with naïve osteochondral constructs were placed into the microfluidic plate as shown in Figure 1. Chondrogenic medium (CM) was supplied through the upper conduit, while osteogenic medium (OM) through the bottom conduit at a flow rate of 1 μ L/s. The following formulas were used for the differentiation media: OM (GM supplemented with 10 ng/mL BMP-2 (PeproTech, Rocky Hill, NJ), 1% L-alanyl-L-glutamine (GlutaMAX), 10 nM dexamethasone (Dex), 0.1 mM L-ascorbic acid 2-phosphate (AsA2-P), and 10 mM beta-glycerophosphate (β -GP); CM (DMEM supplemented with 10 ng/mL TGF- β 3 (PeproTech), 1% ITS, 50 μ M AsA2-P, 55 μ M sodium pyruvate, and 23 μ M L-proline). The perfusion rate was 1 μ L/min, and used syringes were replaced with syringes and new medium every 3 days. After 4 weeks of differentiation, engineered osteochondral tissues were collected for validation using real-time PCR and histological analysis, or treated with IL1-1 β .

Table 1. Primer Sequences for the Genes Analyzed in Real-Time PCR^a

	forward (5'–3')	reverse (5'–3')
SOX9	AGCCTGCGCTCCAATGACT	TAATGGAACACGATGCCTTTCA
ACN	GGCAATAGCAGGTTACAGTACA	CGATAACAGTCTTGCCCCACTT
Col2	TTCCGCGACGTGGACAT	TCAAACCTCGTTGACATCGAAGGT
RUNX2	CAACCACAGAACCACAAAGTGCG	TGTTTGATGCCATAGTCCCTCC
OCN	TCACACTCCTCGCCCTATTG	GAAGAGGAAAGAAGGGTGCC
BSP II	GCAGTAGTGACTCATCCGAAGAA	GCCTCAGAGTCTTCATCTTCATTC
18S	GTAACCCGTTGAACCCCAT	CCATCCAATCGGTAGTAGCG

^aAggrecan (ACN), collagen type II (Col2), Runt-related transcription factor 2 (RUNX2), Osteocalcin (OCN), Bone sialoprotein II (BSP II), and 18S rRNA (18S).

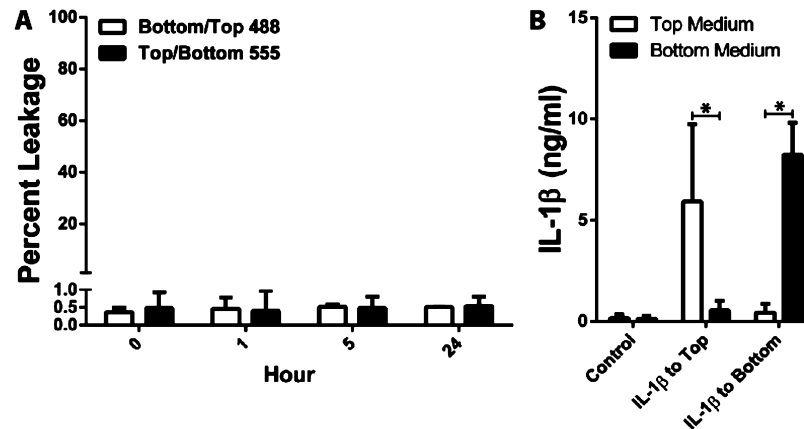


Figure 2. Bioreactor system leak test. (A) Trypsin inhibitor-488 and BSA-555 were simultaneously perfused through the top and bottom space of bioreactor, respectively, and the percent leakage at different time was estimated based on the bottom/top ratio of 488 nm fluorescence readings (bottom/top 488) and top/bottom 555 nm fluorescence readings (top/bottom 555). (B) IL-1 β was included in top or bottom stream and perfused for 24 h. Its concentration in top or bottom medium was then measured. There was statistical difference of IL-1 β concentration in top and bottom medium. * $p < 0.05$.

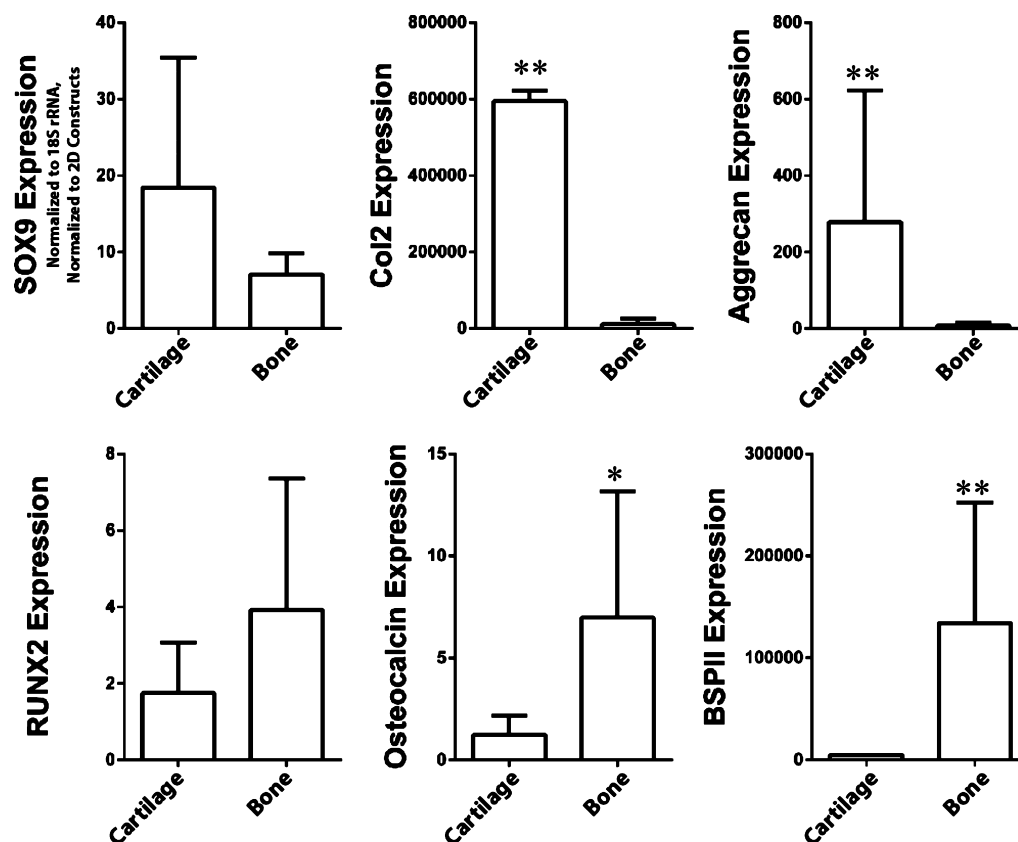


Figure 3. Expression of cartilage and bone markers in the engineered osteochondral construct. After 4 weeks of culture in the bioreactor, osteochondral constructs were separated into chondral (cartilage) and osseous (bone) components, and each were analyzed for expression of cartilage (Sox9, col2, and Aggrecan) or bone (RUNX2, Osteocalcin, BSP II) markers. Expression levels are normalized to 18S rRNA and then to corresponding 2D control expression levels. Expression of cartilage markers was found only in the chondral component, and bone markers in the osseous compartment. * $p < 0.05$; ** $p < 0.01$).

Real-Time PCR. Chondral and osseous constructs were collected separately. To avoid the potential contamination, the bonded margin of each construct was cut away using a razor blade. Total RNA was extracted using Trizol (Invitrogen) following the standard protocol and purified with the RNeasy Plus mini kit (Qiagen, Hilden, Germany). SuperScript III kit (Invitrogen) was utilized with random hexamer primers to

complete the reverse transcription. Real-time RT-PCR was performed using the StepOnePlus thermocycler (Applied Biosystems, Foster City, CA) and SYBR Green Reaction Mix (Applied Biosystems). Sox 9, Aggrecan (ACN), collagen type II (COL2A1), RunX2, Osteocalcin (OCN), and bone sialoprotein (BSP II) expression were analyzed, and primer sequences are listed in Table 1. Monolayers of hBMSCs cultured in GM on

2D tissue culture plastic were used as negative controls. Transcript level of 18S rRNA was used as endogenous control, and gene expression folder changes were calculated using the comparative CT ($\Delta\Delta$ CT) method.

Histological Analysis. Intact engineered osteochondral tissues were fixed in 10% neutral buffered formalin (Fisher Scientific, Pittsburgh, PA) for 7 days, dehydrated, embedded in paraffin with 10 μ m sections cut from each sample. Safranin O/fast green and Alizarin Red staining were used to detect the GAG and calcium deposition, respectively.

IL-1 β Treatment in Engineered Micro-Osteochondral Constructs. After 4 weeks of differentiation, engineered osteochondral constructs were treated with IL-1 β (10 ng/mL, R&D) on the chondral or osseous sides only to investigate the cell/neo-tissue response to pro-inflammatory cytokines and possible communication through the osteochondral construct. The media used in this test were CM without TGF- β 3 (chondral) and OM without BMP-2 (osseous), both supplemented with 10 ng/mL IL-1 β . There were three experimental groups: (1) CM/OM, (2) CM + IL-1 β /OM, and (3) CM/OM + IL-1 β . The treatment lasted 7 days, with effluent medium collected and frozen at 1 and 7 days for ELISA. After 7 days, the osteochondral constructs were bisected into the chondral and osseous halves and processed for gene expression analysis as described before. In addition to tissue specific gene expression, matrix metalloproteinase 1, 3, and 13 were also analyzed.

Enzyme-Linked Immunosorbent Assay (ELISA). Media was collected separately from chondral and osseous constructs, cleared of cell debris via centrifugation (1000g), and analyzed via IL-1 β (Abcam, Cambridge, MA), MMP-1 (R&D), MMP-3 (Abcam, Cambridge, MA), and MMP-13 (Abcam) ELISAs according to the manufacturers' instructions.

Statistical Analysis. Results are expressed as mean \pm standard deviation (SD). Significant differences were determined with ANOVA followed by a Bonferroni post hoc analysis for multiple group comparisons using SPSS Statistics 21 (IBM, Armonk, NY). Significance was determined at $p < 0.05$ (*) and $p < 0.01$ (**).

RESULTS

Bioreactor System Leak Test. The robustness of the microbioreactor was tested by assessing the extent of leakage of two molecules perfused independently in the upper and lower medium conduits: (1) trypsin inhibitor (21 kDa), with a molecular weight similar to the two commonly used osteoinductive (BMP-2, 26kd) and chondroinductive (TGF β 3, 25kd) factors, and (2) BSA (65kd), the most abundant protein in serum. As shown in Figure 2A, after 24 h of perfusion, the extent of mixing between top and bottom was <1%, indicating there was minimal medium exchange through the interfaces between the chamber wall and the inset and between the inset and scaffold-only construct. These results were further confirmed by ELISA assay for IL-1 β in both medium conduits during the IL-1 β test (Figure 2B).

Differentiation of Engineered Osteochondral Construct. The naive hBMSCs seeded within tissue-specific scaffolds in the freshly fabricated osteochondral construct were induced to differentiate using CM in the top stream and OM in the bottom stream. We anticipated chondrogenesis in the upper, chondral half of the construct and osteogenesis in the bottom, osseous half. After 4 weeks of differentiation, biphasic osteochondral constructs were produced (Figure 4C).

As shown in Figure 3, cells in the chondral half showed enhanced expression of chondrogenic genes, including Sox 9, aggrecan, and collagen type II as compared to those in the osseous half, while the cells in the osseous half had higher expression of osteogenic genes, including RunX2, osteocalcin, and BSP II. Monolayers of hBMSCs cultured in GM on 2D tissue culture plastic were used as negative controls. Histological staining with Alcian Blue/Alizarin Red revealed high matrix GAG content in the upper chondral half than the osseous half (Figure 4B); although the amount of calcium

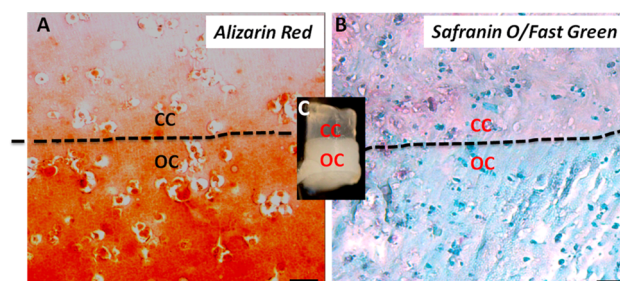


Figure 4. Histology of the engineered osteochondral construct. Top, chondral component (CC); bottom, osseous component (OC). (A) Alizarin Red staining; (B) Safranin O/fast green staining. Dashed lines indicate the border between CC and OC. Scale bar = 100 μ m. (C) Macroscopic view of the engineered osteochondral construct.

deposition in the osseous half was not detectable. Taken together, these results strongly indicate a spatially defined, biphasic differentiation of these engineered osteochondral constructs, with the chondral component undergoing more characteristic differentiation. In addition, H&E staining revealed a distinct, <100 μ m wide basophilic band in the interface between the chondral and osseous halves, potentially indicative of a developing tidemark (Figure 4A).

IL-1 β Treatment on Engineered Osteochondral Tissue. As described above, the microtissue bioreactor presented here, with its two separate medium flow systems and biphasic construct compartments, has the capability for targeted treatment of one (or both) tissue construct(s) with soluble factors. Osseous and chondral components were separately treated with the pro-inflammatory cytokine IL-1 β (10 ng/mL) for 7 days (control conditions consisted of untreated osteochondral constructs), and the responses of each of the two components were separately analyzed. Media samples were collected from chondral and osseous components streams at days 1 and 7, and after day 7, the osteochondral constructs were separated into osseous and chondral components, and each was separately analyzed for gene expression of catabolic genes (MMP-1, MMP-3, and MMP-13) and either cartilage markers (Sox9, Col2, and Aggrecan) (Figure 5) or bone markers (RUNX2, Osteocalcin, and BSP II) (Figure 6). Media samples from the chondral and osseous components stream collected at days 1 and 7 were analyzed via MMP-1, MMP-3, and MMP-13 ELISAs (Figure 7).

Treatment of chondral constructs with IL-1 β caused decreases in expression of cartilage genes Sox9, Col2, and Aggrecan, consistent with physiological outcomes of damaged or stressed cartilage (Figure 5). Chondral construct expression of these genes also decreased in response to IL-1 β treatment of osseous constructs, suggesting signaling between the osseous and chondral components. Evidence of this osseous-to-chondral communication was even more apparent in results

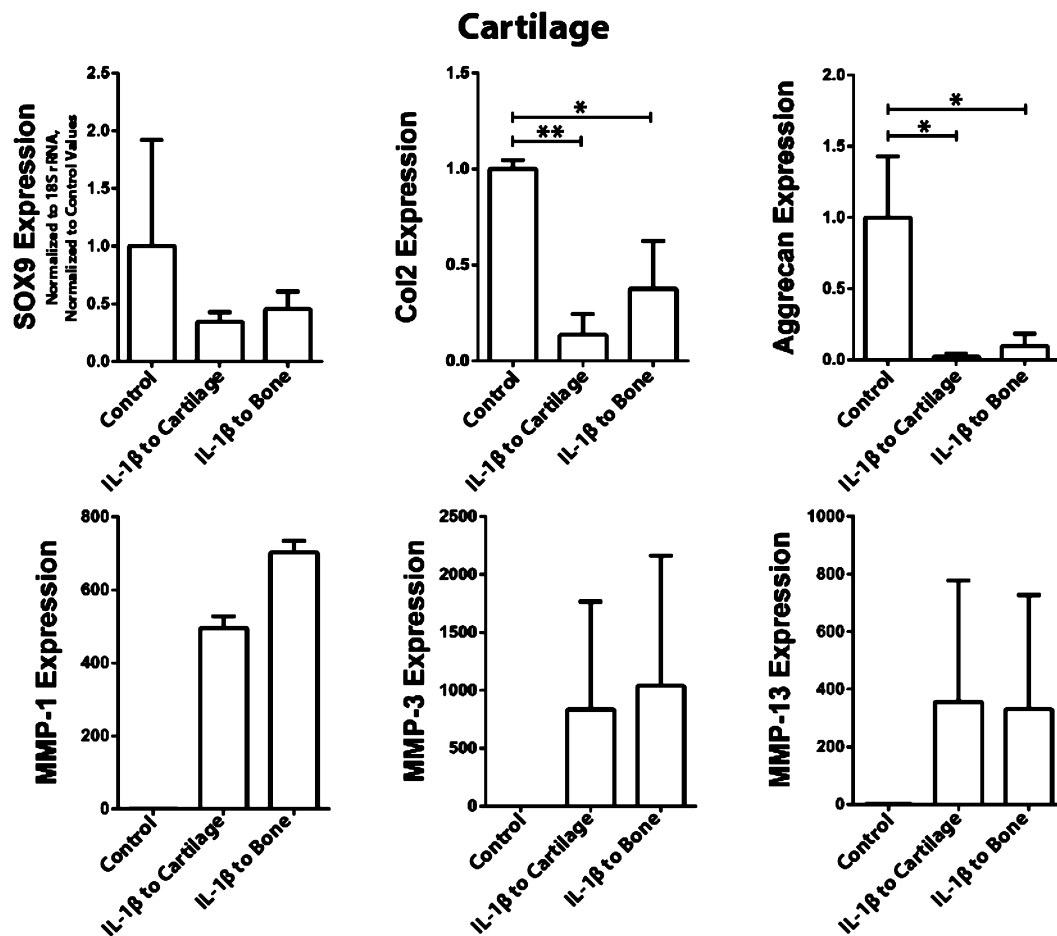


Figure 5. Effects of IL-1 β treatment on cartilage gene expression in the engineered osteochondral microtissue. After treatment of either osseous (bone) or chondral (cartilage) component with 10 ng/mL IL-1 β for 7 days, cartilage components were analyzed for the expression of cartilage markers and MMPs. Untreated constructs were used as controls. Expression levels were normalized to 18S rRNA expression and then to corresponding gene expression under control conditions. * $p < 0.05$; ** $p < 0.01$.

concerning expression of catabolic genes; expression of MMP-1, MMP-3, and MMP-13 of the chondral constructs increased substantially in response to IL-1 β treatment of the osseous component. Crosstalk between the two components was also detected in the case of chondral-to-osseous communication (Figure 6). IL-1 β treatment of the chondral construct caused decreases in expression of the bone genes osteocalcin and BSP1I and increases in MMPs production in the osseous construct, particularly MMP-13, which is one of the most important mediators of OA cartilage degradation.

ELISA analysis of MMPs secreted by the chondral and osseous components at different time points allowed for observations on the rate of signal propagation between the two components (Figure 7). For example, the chondral construct responded to IL-1 β treatment of the osseous component with increases in MMP-1, MMP-3, and MMP-13 secretion. The chondral MMP-13 response occurred quickly, within 1 day, while the chondral MMP-1 response took 7 days. The chondral MMP-3 response time was intermediate between those of MMP-13 and MMP-1. Again, these results are interesting considering the central role MMP-13 plays in cartilage degeneration. The osseous construct response to treatment of chondral component with IL-1 β , however, was quick yet increased further over time, and by day 7 was overall stronger than the chondral responses to the osseous component treatment.

It is worth noting that gene expression and protein levels of MMPs should not be expected to be necessarily consistent. This stems from differences in the ways in which ELISA and real-time PCR samples were collected and measured. ELISA samples consisted of culture media conditioned by cells for 24 h and were collected at day 1 or day 7 for each experiment. The proteins contained in day 1 samples were secreted between days 0 and 1, and day 7 samples contained proteins secreted between days 6 and 7. PCR samples, however, were collected after 7 days of cultures and represent the expressional activities taking place at the moment of collection. In other words, the mRNA levels analyzed by PCR at day 7 are not necessarily totally reflective of the protein levels analyzed by ELISA in day 7 conditioned media samples. This disconnect between PCR and ELISA measurements may be more pronounced in MMPs, which need to be translated, secreted, and then diffuse out of the 3D construct before they are detected by ELISA. Furthermore, differences between PCR and ELISA values also arise from differences in normalization. PCR results are normalized to 18S rRNA expression, thereby taking into account cell number. ELISA results are instead a representation of the entire culture and normalized to control conditions. Thus, any experimental treatment that may affect cell number would have a larger impact on ELISA results than PCR results. Since chondrocytes are particularly sensitive to IL-1 β , this may explain why results concerning cells of the chondral component

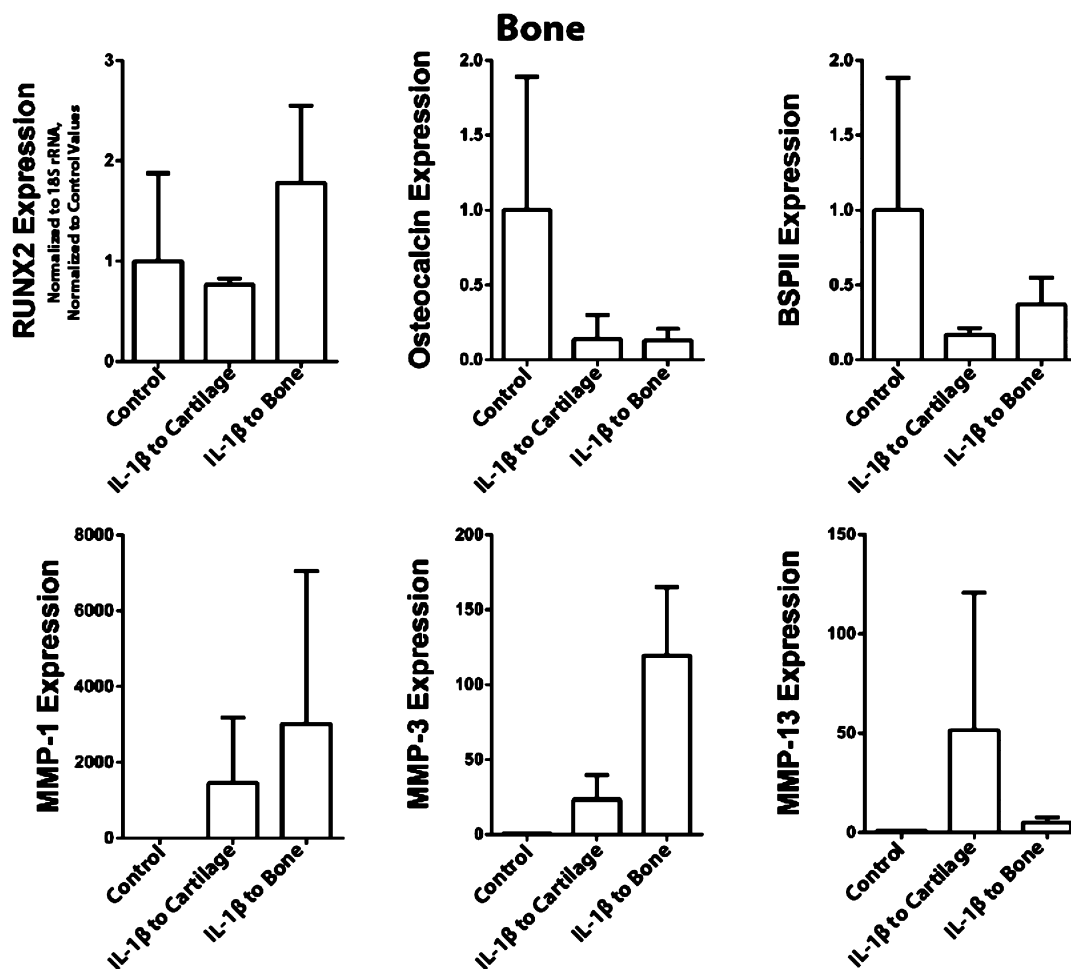


Figure 6. Effects of IL-1 β treatment on bone gene expression in the engineered osteochondral microtissue. After treatment of either osseous (bone) or chondral (cartilage) component with 10 ng/mL IL-1 β for 7 days, bone components were analyzed for expression of bone markers and MMPs. Untreated samples were used as controls. Expression levels were normalized to 18S rRNA expression and then to corresponding gene expression under control conditions.

exhibit the greatest degree of inconsistency between PCR and ELISA measurements when chondral constructs are directly stimulated by IL-1 β .

DISCUSSION

In this study, we have developed a novel bioreactor system for the engineering of osteochondral tissue. RT-PCR and histological analyses showed that hBMSCs-derived naïve constructs have been successfully differentiated into cartilage-like tissue on the top and bone-like tissue on the bottom, using separated culture medium for 4 weeks. A transition layer between 2 tissues is also observed. We then further test the response of engineered osteochondral tissue to IL-1 β treatment. Our results show that IL-1 β exposure decreases the ECM anabolic gene expression but greatly enhances the levels of MMP expression and secreted amount into the medium. Interestingly, the IL-1 β insulted osseous construct induces a catabolic gene expression response into the untreated chondral component, which is not due to leakage of IL-1 β , suggesting active osseous–chondral interaction and the likely importance of bone injury in OA development.

In this study, a dual-chamber bioreactor has been developed to generate and maintain osteochondral constructs derived from human hBMSCs. The design parameters included

individual compartments to separate the chondral and osseous microenvironments that are individually accessible for the introduction of bioactive agents and/or candidate effector cells, tissue and medium sampling, and compositional assays, including noninvasive imaging techniques. Furthermore, the total dimension and geometry of the bioreactor matches that of a multiwell culture plate chamber for the development of medium- to high-throughput analysis. Validation of the system included successful, simultaneous differentiation of osseous and chondral constructs from hBMSCs from the same source (pooling of three donors) and subsequent application of IL-1 β , a potent inflammatory mediator implicated in OA pathophysiology, to test the physiological response of the osteochondral construct.

We have shown that in the course of 6 weeks, hBMSCs undergo tissue-specific differentiation in response to the tissue specific growth media and hydrogel composition provided. The differentiating bBMSCs expressed tissue-specific transcription factors and ECM molecules, as shown by RT-PCR and histological staining. Most impressively, there was an indication of a basophilic, tidemark-like zone separating the chondral and osseous components. This region is quite broad and therefore not an artifact. We believe this shows a biochemically relevant, “anabolic” or “homeostatic” interaction between the chondral and osseous components. The recreation of the a tidemark-

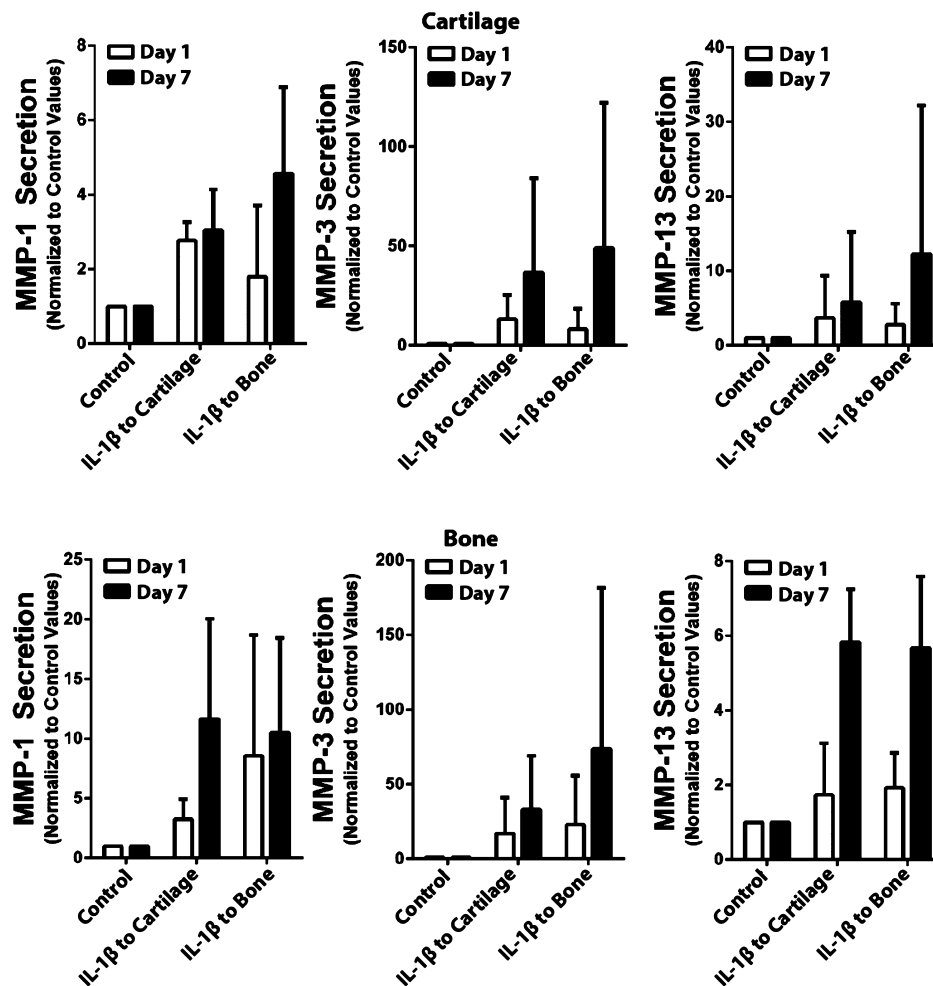


Figure 7. Effects of IL-1 β treatment on osseous and chondral MMP secretion in the engineered osteochondral microtissue. After treatment of either osseous (bone) or chondral (cartilage) component with 10 ng/mL IL-1 β for 1 or 7 days, medium samples collected from the bone or cartilage medium compartment were analyzed by ELISA for the levels of secreted MMP-1, MMP-3, and MMP-13. Values were normalized to those measured under control conditions, which involved untreated osteochondral constructs.

containing biphasic tissue is vital to drug testing using an osteochondral organotypic culture since changes in the OCJ are mechanistically involved in OA progression and likely to be a target of toxicants and DMOADs.²⁴

We subsequently tested the response of the MSC-based osteochondral tissue to IL-1 β . The test served two purposes: (1) to validate the utility of the bioreactor in osteochondral studies and (2) to assess the physiological replication of the OC tissue by the MSCs in this bioreactor. Specifically, we sought detectable communication between the tissues. IL-1 β is almost ubiquitous in inflammatory diseases, is prominent in advanced OA in both the cartilage and synovial lining, and is frequently employed as a pathogenic initiator in *in vitro* models of OA.^{25,26} Application of IL-1 β to both osseous and chondral components results in clear matrix degeneration and phenotypic changes in the resident cells, similar to what has been observed in monocultures of chondrocytes and osteoblasts.^{27,28} How to apply the IL-1 β to an osteochondral construct remains an open question. While chronic degeneration of the articular surface is most prevalent in OA, it is not clear whether alterations in the subchondral bone or articular cartilage is the primary trigger in OA. Using the bioreactor in this study, we are able to study interactions between cartilage and bone that may contribute to OA progression

Clear osseous and chondral tissue interactions are observed when IL-1 β is applied to the osseous component, which results in low levels of anabolic gene expression (SOX9, Col2, and Aggrecan) but robust expression of MMPs in the cartilage component. The MMP expression patterns are further validated by ELISAs. Conversely, application of IL-1 β to the cartilage induces in bone low levels of anabolic bone gene expression (Runx2, OPN, and BSP1) but robust expression of MMPs. This apparently contradictory simultaneous induction of anabolic and catabolic processes within a tissue is entirely in keeping with the hypothesis that OA begins initially with a shift in the balance between anabolic and catabolic activities, followed by phenotypic changes in the cells in response to the modified environment.^{29,30} To some degree, inflammation can have beneficial effects on tissues, but at higher concentrations, inflammatory mediators induce tissue remodeling/destruction.³¹ Focusing on the response of chondral component to IL-1 β treatment of the osseous component, it is interesting that direct application of IL-1 β to the chondral component has a less impressive catabolic response than indirect exposure via the osseous component. This result implies that the affected osteoblasts in the osseous component are producing bioactive factors, in addition to IL-1 β , that are causing greater catabolic responses than IL-1 β itself and vice

versa. Further, it shows that there is biochemically relevant “degenerative” communication between the cartilage and the bone.

The formation of an OCJ between regions of engineered cartilage and bone is often reported, but generally is not analyzed beyond histological identification. In our study, we have employed opposing chondrogenic and osteogenic nutrient gradients to stimulate OCJ formation by naïve, differentiating MSCs. It is thus difficult to relate the potential tidemark development in our construct with frequently reported constructs that combine solid, porous polymeric sponges and hydrogels for osteochondral engineering *in vitro* or *in vivo* because of the great disparity in tissue architecture and scaffold biochemistry.³² Tidemark development similar to what is seen here has been reported in studies employing microparticle-mediated spatially restricted growth factor release, microbead-encapsulated MSC-derived chondrocytes and osteocytes, MSCs encapsulated within scaffold material gradients,^{33–35} and MSCs stimulated by growth factor gradients.³⁶ In all cases, the basophilic tidemark is indistinct and broad, particularly in models without loading. We expect that appropriate mechanical loading and enhancement of cell differentiation, e.g., with an oxygen gradient, may enhance the collection of metabolites to form the tidemark at the deep zone/calcified cartilage interface, particularly if differentiation is enhanced with an oxygen gradient and/or the addition of hydroxyapatite.

While formation of OCJ has been reported in *in vivo* implanted cell-seeded scaffold,^{37,38} there have been relatively few studies using a controlled bioreactor as reported here. The features of our bioreactor design, including separate compartments for the “chondral” and “osseous” microenvironments supplied by independent tissue-specific media that can be controlled and regulated via introductions of bioactive agents or candidate effector cells, and capability of individual sampling of the different compartments, are thus of potential value in allowing more individual manipulations. Specifically, we envision its application for the assessment of drug and environmental factor toxicity. We have postulated that catabolic insults to one tissue component comprising the osteochondral unit would influence the other in a manner reminiscent of tissue degeneration in OA. Of particular interest is to investigate the communication of biomechanical signals/forces. To our knowledge, we are the first to provide evidence of communication between different compartments of an osteochondral construct in response to catabolic cues (IL-1 β). The tissue responses reported here reflect a subset of pathophysiological conditions reported in *in vitro* and *in vivo* models of OA. IL-1 β is utilized in models of both rheumatoid and OA, with the effect of causing cartilage matrix breakdown and down regulation of cartilage matrix gene expression as shown here. In contrast, IL-1 β has been reported to induce increased bone matrix deposition, although it is a matrix of inferior quality,^{26,29} which may explain the response of the osseous component to direct exposure to IL-1 β in our model. The fact that catabolic gene expression in the osseous component is more enhanced by exposure of the overlying chondral component to IL-1 β suggests that the chondral construct is producing additional signals and catabolic factors that travel to and affect the osseous component below, possibly constituting a form of intercellular communication not previously reported.

In summary, we have fabricated a new microfluidic-based, multichamber bioreactor for osteochondral differentiation and

toxicity testing. We demonstrated clear biphasic tissue differentiation in response to opposing chondrogenic and osteogenic gradients produced by tissue-specific differentiation factors supplied by independent medium streams to the chondral and osseous components of the construct. Finally we have shown that MSC-based chondral and osseous tissues are capable of responding to IL-1 β in a relevant manner and that changes in one tissue compartment are communicated, and perhaps amplified, to the other along the osteochondral axis. This bioreactor/organotypic osteochondral culture combination will enable us to focus on the relationship of cartilage and bone in growth and degeneration and perhaps help to elucidate the roles of each tissue in OA. Finally, with minimal modification and appropriate coupling, the bioreactor reported here can be adapted as a tissue-specific component of an interacting multitissue bioreactor platform to study systemic multitissue interactions.

AUTHOR INFORMATION

Corresponding Author

*(R.S.T.) Phone: 4126482603. Fax: 4126245544. E-mail: rst13@pitt.edu.

Author Contributions

[§]These authors (H.L., T.P.L., and P.G.A.) contributed equally to this work.

Notes

The authors declare no competing financial interest.

ACKNOWLEDGMENTS

The authors gratefully thank Dr. Jian Tan for the preparation of the hBMSCs. This work is supported in part by the National Institutes of Health (U18TR000532), the Commonwealth of Pennsylvania Department of Health (SAP4100050913), the U.S. Department of Defense (W81XWH-08-2-0032 and W81XWH-10-1-0850), and the Ri.MED Foundation (Italy).

REFERENCES

- (1) Goldring, M. B. Update on the biology of the chondrocyte and new approaches to treating cartilage diseases. *Best Pract. Res., Clin. Rheumatol.* **2006**, *20*, 1003–1025.
- (2) Lethbridge-Cejku, M.; Helmick, C. G.; Popovic, J. R. Hospitalizations for arthritis and other rheumatic conditions: Data from the 1997 National Hospital Discharge Survey. *Med. Care.* **2003**, *41*, 1367–1373.
- (3) Schaible, H. G. Mechanisms of chronic pain in osteoarthritis. *Curr. Rheumatol. Rep.* **2012**, *14*, 549–556.
- (4) Spiller, K. L.; Maher, S. A.; Lowman, A. M. Hydrogels for the repair of articular cartilage defects. *Tissue Eng., Part B* **2011**, *17*, 281–299.
- (5) Henrotin, Y.; Pesesse, L.; Sanchez, C. Subchondral bone and osteoarthritis: biological and cellular aspects. *Osteoporosis Int.* **2012**, *23*, S847–S851.
- (6) Ciani, C.; Doty, S. B.; Fritton, S. P. An effective histological staining process to visualize bone interstitial fluid space using confocal microscopy. *Bone* **2009**, *44*, 1015–1017.
- (7) Fritton, S. P.; Weinbaum, S. Fluid and solute transport in bone: Flow-induced mechanotransduction. *Annu. Rev. Fluid Mech.* **2009**, *41*, 347–374.
- (8) Nukavarapu, S. P.; Dorcenus, D. L. Osteochondral tissue engineering: Current strategies and challenges. *Biotechnol Adv.* **2013**, *31*, 706–721.
- (9) Pan, J.; Zhou, X. Z.; Li, W.; Novotny, J. E.; Doty, S. B.; Wang, L. Y. In situ measurement of transport between subchondral bone and articular cartilage. *J. Orthop. Res.* **2009**, *27*, 1347–1352.

- (10) Pan, J.; Wang, B.; Li, W.; Zhou, X. Z.; Scherr, T.; Yang, Y. Y.; Price, C.; Wang, L. Y. Elevated cross-talk between subchondral bone and cartilage in osteoarthritic joints. *Bone* **2012**, *51*, 212–217.
- (11) Fermor, B.; Christensen, S. E.; Youn, I.; Cernanec, J. M.; Davies, C. M.; Weinberg, B. Oxygen, nitric oxide and articular cartilage. *Eur. Cells Mater.* **2007**, *13*, 56–65.
- (12) Lafont, J. E. Lack of oxygen in articular cartilage: consequences for chondrocyte biology. *Int. J. Exp. Pathol.* **2010**, *91*, 99–106.
- (13) van Driel, M.; van Leeuwen, J. P. Vitamin D endocrine system and osteoblasts. *Bonekey Rep.* **2014**, *3*, 493.
- (14) Park, J. B. The effects of dexamethasone, ascorbic acid, and beta-glycerophosphate on osteoblastic differentiation by regulating estrogen receptor and osteopontin expression. *J. Surg. Res.* **2012**, *173*, 99–104.
- (15) Poole, A. R.; Rizkalla, G.; Ionescu, M.; Reiner, A.; Brooks, E.; Rorabeck, C.; Bourne, R.; Bogoch, E. Osteoarthritis in the human knee: a dynamic process of cartilage matrix degradation, synthesis and reorganization. *Agents Actions Suppl.* **1993**, *39*, 3–13.
- (16) Guilak, F. Biomechanical factors in osteoarthritis. *Best Pract. Res. Clin. Rheumatol.* **2011**, *25*, 815–823.
- (17) de Vries-van Melle, M. L.; Mandl, E. W.; Kops, N.; Koevoet, W. J. L. M.; Verhaar, J. A. N.; van Osch, G. J. V. M. An osteochondral culture model to study mechanisms involved in articular cartilage repair. *Tissue Eng., Part C* **2012**, *18*, 45–53.
- (18) Loores, R. J.; Luyten, F. P. The bone-cartilage unit in osteoarthritis. *Nat. Rev. Rheumatol.* **2011**, *7*, 43–49.
- (19) Lin, H.; Cheng, A. W.; Alexander, P. G.; Beck, A. M.; Tuan, R. S. Cartilage tissue engineering application of injectable gelatin hydrogel with in situ visible-light-activated gelation capability in both air and aqueous solution. *Tissue Eng., Part A* **2014**, DOI: 10.1089/ten.tea.2013.0642.
- (20) Fairbanks, B. D.; Schwartz, M. P.; Bowman, C. N.; Anseth, K. S. Photoinitiated polymerization of PEG-diacrylate with lithium phenyl-2,4,6-trimethylbenzoylphosphinate: polymerization rate and cytocompatibility. *Biomaterials* **2009**, *30*, 6702–6707.
- (21) Van den Bulcke, A. I.; Bogdanov, B.; De Rooze, N.; Schacht, E. H.; Cornelissen, M.; Berghmans, H. Structural and rheological properties of methacrylamide modified gelatin hydrogels. *Biomacromolecules* **2000**, *1*, 31–38.
- (22) Nichol, J. W.; Koshy, S. T.; Bae, H.; Hwang, C. M.; Yamanlar, S.; Khademhosseini, A. Cell-laden microengineered gelatin methacrylate hydrogels. *Biomaterials* **2010**, *31*, 5536–5544.
- (23) Chung, C.; Beecham, M.; Mauck, R. L.; Burdick, J. A. The influence of degradation characteristics of hyaluronic acid hydrogels on in vitro neocartilage formation by mesenchymal stem cells. *Biomaterials* **2009**, *30*, 4287–4296.
- (24) Suri, S.; Walsh, D. A. Osteochondral alterations in osteoarthritis. *Bone* **2012**, *51*, 204–211.
- (25) Goldring, M. B.; Otero, M.; Tsuchimochi, K.; Ijiri, K.; Li, Y. Defining the roles of inflammatory and anabolic cytokines in cartilage metabolism. *Ann. Rheum. Dis.* **2008**, *67* (Suppl 3), iii75–82.
- (26) Kapoor, M.; Martel-Pelletier, J.; Lajeunesse, D.; Pelletier, J. P.; Fahmi, H. Role of proinflammatory cytokines in the pathophysiology of osteoarthritis. *Nat. Rev. Rheumatol.* **2011**, *7*, 33–42.
- (27) Page, C. E.; Smale, S.; Carty, S. M.; Amos, N.; Lauder, S. N.; Goodfellow, R. M.; Richards, P. J.; Jones, S. A.; Topley, N.; Williams, A. S. Interferon-gamma inhibits interleukin-1 beta-induced matrix metalloproteinase production by synovial fibroblasts and protects articular cartilage in early arthritis. *Arthritis Res. Ther.* **2010**, *12*, R49.
- (28) Fujisaki, K.; Tanabe, N.; Suzuki, N.; Mitsui, N.; Oka, H.; Ito, K.; Maeno, M. The effect of IL-1 alpha on the expression of matrix metalloproteinases, plasminogen activators, and their inhibitors in osteoblastic ROS 17/2.8 cells. *Life Sci.* **2006**, *78*, 1975–1982.
- (29) Clements, K. M.; Price, J. S.; Chambers, M. G.; Visco, D. M.; Poole, A. R.; Mason, R. M. Gene deletion of either interleukin-1beta, interleukin-1beta-converting enzyme, inducible nitric oxide synthase, or stromelysin 1 accelerates the development of knee osteoarthritis in mice after surgical transection of the medial collateral ligament and partial medial meniscectomy. *Arthritis Rheum.* **2003**, *48*, 3452–3463.
- (30) Mueller, M. B.; Tuan, R. S. Anabolic/catabolic balance in pathogenesis of osteoarthritis: identifying molecular targets. *PM&R* **2011**, *3*, S3–11.
- (31) Williams, E. L.; Edwards, C. J.; Cooper, C.; Oreffo, R. O. C. Impact of inflammation on the osteoarthritic niche: implications for regenerative medicine. *Regener. Med.* **2012**, *7*, 551–570.
- (32) Vunjak-Novakovic, G.; Meinel, L.; Altman, G.; Kaplan, D. Bioreactor cultivation of osteochondral grafts. *Orthod. Craniofacial Res.* **2005**, *8*, 209–218.
- (33) Dormer, N. H.; Singh, M.; Zhao, L.; Mohan, N.; Berkland, C. J.; Detamore, M. S. Osteochondral interface regeneration of the rabbit knee with macroscopic gradients of bioactive signals. *J. Biomed. Mater. Res. A* **2012**, *100*, 162–170.
- (34) Mohan, N.; Gupta, V.; Sridharan, B.; Sutherland, A.; Detamore, M. S. The potential of encapsulating 'raw materials' in 3D osteochondral gradient scaffolds. *Biotechnol. Bioeng.* **2013**, *111*, 829–841.
- (35) Nguyen, L. H.; Kudva, A. K.; Saxena, N. S.; Roy, K. Engineering articular cartilage with spatially-varying matrix composition and mechanical properties from a single stem cell population using a multi-layered hydrogel. *Biomaterials* **2011**, *32*, 6946–6952.
- (36) Shi, X.; Zhou, J.; Zhao, Y.; Li, L.; Wu, H. Gradient-regulated hydrogel for interface tissue engineering: steering simultaneous osteo/chondrogenesis of stem cells on a chip. *Adv. Healthcare Mater.* **2013**, *2*, 846–853.
- (37) Da, H.; Jia, S. J.; Meng, G. L.; Cheng, J. H.; Zhou, W.; Xiong, Z.; Mu, Y. J.; Liu, J. The impact of compact layer in biphasic scaffold on osteochondral tissue engineering. *PLoS One* **2013**, *8*, e54838.
- (38) Saha, S.; Kundu, B.; Kirkham, J.; Wood, D.; Kundu, S. C.; Yang, X. B. Osteochondral tissue engineering in vivo: A comparative study using layered silk fibroin scaffolds from mulberry and nonmulberry silkworms. *PLoS One* **2013**, *8*, e80004.